

# Synthesis Technology of Magnesium-Doped Nanometer Hydroxyapatite: A Review

Kui Zhang, Yan Liu, Zhenrui Zhao, Xuwen Shi, Ruihao Zhang, Yixiang He, Huaibin Zhang, Yi Sun, and Wenji Wang\*

Cite This: *ACS Omega* 2023, 8, 44458–44471

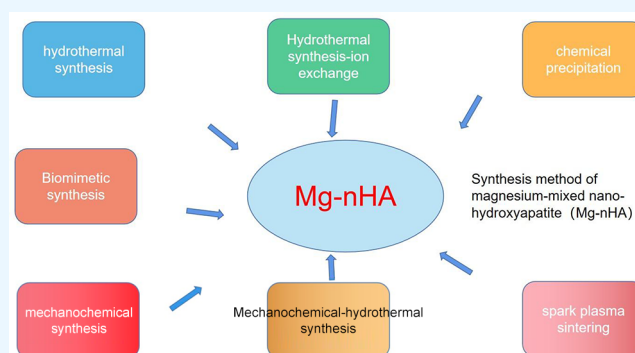
Read Online

ACCESS |

Metrics & More

Article Recommendations

**ABSTRACT:** Ion substitution techniques for nanoparticles have become an important neighborhood of biomedical engineering and have led to the development of innovative bioactive materials for health systems. Magnesium-doped nanohydroxyapatite (Mg-nHA) has good bone conductivity, biological activity, flexural strength, and fracture toughness due to particle doping technology, making it an ideal candidate material for biomedical applications. In this Review, we have systematically presented the synthesis methods of Mg-nHA and their application in the field of biomedical science and highlighted the pros and cons of each method. Finally, some future prospects for this important neighborhood are proposed. The purpose of this Review is to provide readers with an understanding of this new field of research on bioactive materials with innovative functions and systematically introduce the latest technologies for obtaining uniform, continuous, and morphologically diverse Mg-nHA.



latest technologies for obtaining uniform, continuous, and morphologically diverse Mg-nHA.

## 1. INTRODUCTION

Each year, a large number of people suffer from infections, bone tumors, osteoporosis, various accidents, and other issues, resulting in varying degrees of bone defects that severely affects the lives of the patients and their physical and mental health.<sup>1–3</sup> One of the main treatments for a lot of bone loss is the use of biomaterials as bone implants.<sup>4–6</sup> The development of biomaterials with structural properties and functions similar to those of natural bone, such as mechanical strength, bone integration, thermal stability, and antibacterial capabilities, has received much attention.<sup>7–9</sup> These studies have helped replace autologous bone with bone substitute materials and are believed in to be one of a growing number of activities for human tissue replacement surgery. Current biological materials have certain limitations, so the development direction of bone replacement materials is to explore a novel bone repair material, optimize the function and structure of the materials, and improve the preparation methods of the materials to improve their biocompatibility, biological activity, and mechanical properties.<sup>9,10</sup> For example, magnesium-doped nanohydroxyapatite (Mg-nHA) is a biologically superior bone substitute material.<sup>11–13</sup>

Magnesium (Mg) is one of the most essential elements in the human body, with 60–65% in bones and teeth and 35–40% in the rest of the body.<sup>14–17</sup> Mg<sup>2+</sup> affects bone metabolism, regulates the activity of osteoblasts and

osteoclasts, and stimulates the process of osteogenesis. Moreover, as magnesium is an essential element for the human body, the element itself has no deleterious properties.<sup>18–22</sup> Magnesium-based materials are considered innovative materials for orthopedic implants due to their biocompatibility and biodegradability.<sup>23–26</sup> Magnesium-based materials, however, have some problems. First, magnesium tends to produce hydrogen gas during reactions in the body, creating bubbles in the tissue surrounding the implant.<sup>27–30</sup> This prevents the material from binding to the tissues. Therefore, to make magnesium-containing composites more corrosion-resistant, the hydrogen precipitation rate must be reduced. Numerous scholars have proposed different solutions, such as alloying, coating, and ion substitution, to improve the corrosion resistance of magnesium.<sup>31–33</sup> While bone tissue repair often takes more than three months, magnesium implants lose their mechanical properties within six to nine weeks of implantation.<sup>34–37</sup> As a result, it is challenging to maintain the integrity of the necessary mechanical properties

**Received:** August 17, 2023  
**Revised:** October 20, 2023  
**Accepted:** October 25, 2023  
**Published:** November 13, 2023



**Table 1. Production of Nanohydroxyapatite with Different Sizes and Shapes by Different Preparation Methods**

synthetic strategy	dominance	morphology and size	ref.
	wet synthesis		
sono-chemical	monodispersed nanoparticles of different shapes could be produced	irregular, sphere, filament, rod, tube. monodispersed nanoparticles of different shapes could be produced. size range: 5 nm to 1000 $\mu\text{m}$	65–68
polyol	nonagglomeration, high boiling point of polyols used as the solvent as well as the reducing agent	irregular, leaf, flake, plate, whisker, nanorods. size range: 5 nm to 80 $\mu\text{m}$	65,69,70
microemulsions	better control of particle size, restricted hard agglomeration	irregular, sphere, rod, tube, flower. size range: 5 nm to 8 $\mu\text{m}$	65, 71, 72
hydrothermal synthesis	enhanced solubility of precursors, controlled growth dynamics	irregular, sphere, rod, needle, tube, fiber, wire, whisker, feathery structures. size range: 3 nm to 1000 $\mu\text{m}$	65, 73, 74
sol–gel synthesis	molecular-level mixing of reactants improves the chemical homogeneity of synthesized pure and hybrid nanostructures at low temperatures	irregular, sphere, rod, needle, tube, filament, whisker, platelet. size range: 3 nm to 1000 $\mu\text{m}$	65, 75–77
coprecipitation	simplest and most efficient chemical method. synthesis at room temperature. particle size can easily be controlled by adjusting the pH and ionic strength of reaction media. nanostructures of wide range of sizes and morphologies	irregular, sphere, rod, needle, tube, fiber, filament, wire, whisker, strip, platelet, flower. size range: 3 nm to 1000 $\mu\text{m}$	65, 78, 79
	dry synthesis		
solid state	well crystallized structure	irregular, filament, rod, needle, whisker. size range: 5 nm to 1000 $\mu\text{m}$	65, 80, 81
mechanochemical	no calcination is required	irregular, sphere, rod, needle, whisker. size range: 5 nm to 200 $\mu\text{m}$ .	65, 82, 83
	high-temperature synthesis		
thermal decomposition	good size control, narrow size variation and good crystallinity	irregular, flake, plate, sheet, formless. size range: 5 nm to 200 $\mu\text{m}$	65, 84, 85
combustion	quickly procedure, high purity, single-step operation	sphere, oval, ball, irregular spherical. size range: 5 nm to 200 $\mu\text{m}$	65, 86, 87
pyrolysis	rod-like nanoparticles and single phase with high crystallinity and good stoichiometry	nanorods embedded to micrometer form. size range: 10 nm to 1000 $\mu\text{m}$	65, 88, 89

throughout the healing process. This is necessary to reduce the degradation rate of magnesium-based materials so that they can be used in orthopedic implants.<sup>38–40</sup>

The structure and composition of hydroxyapatite (HA) are similar to those of natural bone. It has excellent biocompatibility and bone conductivity and can form chemical bonds with the bone tissue, which is important in biomedical engineering.<sup>41–45</sup> However, the preparation of porous HA as a scaffold (template) for facilitating bone regeneration and growth has presented a formidable challenge to researchers. The integration of additive manufacturing technology provides the advantage of relatively rapid, precise, controllable, and potentially scalable fabrication processes, thereby opening up novel possibilities in the realm of bioceramic scaffolds.<sup>46</sup>

Nanoscale metal–organic frameworks (nano-MOFs), which are three-dimensional porous nanomaterials composed of metal ions and organic ligands with an infinite lattice structure, represent a cutting-edge additive manufacturing technology. The recent surge in research efforts has been directed toward the utilization of nano-MOFs in tissue engineering applications owing to their distinctive attributes, including tunability, excellent biocompatibility, appropriate size, intracellular accessibility of active sites, and expedited adsorption/desorption kinetics.<sup>47,48</sup> Furthermore, unlike their large-volume counterparts, nano-MOFs offers enhanced capabilities for delivering small materials such as drugs and biomolecules into cells, thereby significantly improving the loading efficiency within scaffolds.<sup>46</sup> The preparation and research progress of a significant opportunity for scaffolds in bone and wound tissue engineering.

The magnesium-doped nanohydroxyapatite-based biomaterials, which are nano-MOF materials, have been extensively utilized in the field of biomedicine. However, we reviewed a large number of relevant experimental research and found that the experimental methods of the magnesium ions mixed in

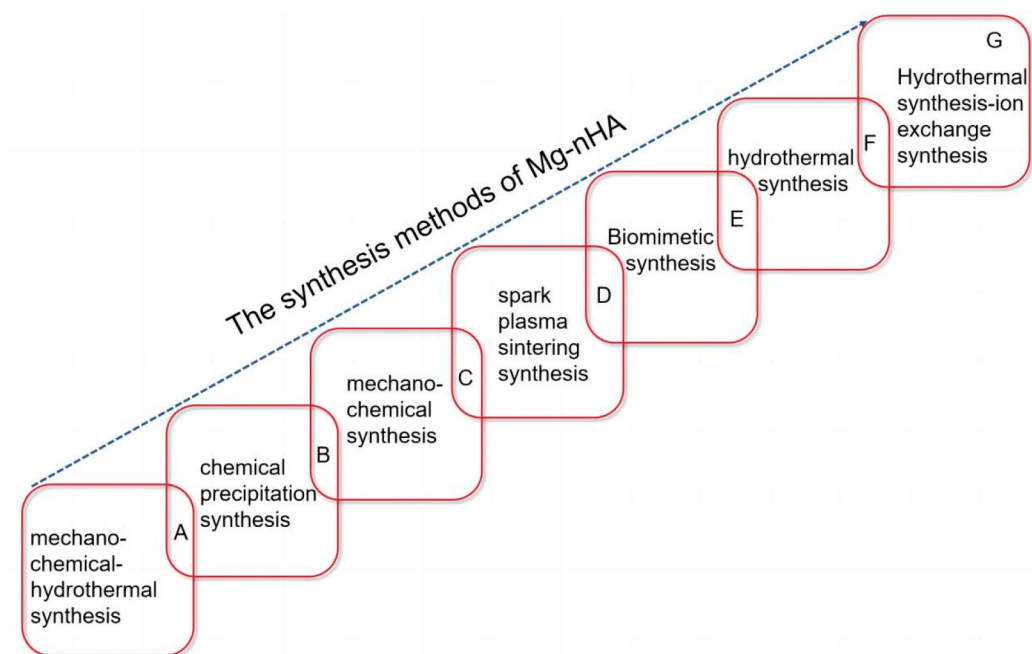
nanohydroxyapatite (nHA) are different, and it was found that there are very few reports on the preparation methods of Mg-nHA crystals and a lack of systematic and complete literature reviews. This Review presents a comprehensive and systematic overview of the preparation methods, biological characterization, and physicochemical properties of Mg-nHA. It encompasses the latest research findings and development trends in related fields while also collating and analyzing numerous literature sources to present key issues, controversies, and potential future research directions. It will provide systematic theoretical and operational guidance for subsequent experimental studies by scholars.

## 2. DOPING OF IONS WITH NANOHYDROXYAPETITE

Optimizing the performance of nHA by doping ions is the best approach. Ion doping commonly includes cation and anion doping in two main ways. Cationic dopants typically include strontium ions, europium ions, terbium ions, and magnesium ions, among others.<sup>49–51</sup> Among them, the strontium ion can improve the biological activity of nHA by changing its ionic shape.<sup>52,53</sup> Additionally, because strontium has multiple radioactive isotopes and selective half-lives, it helps nHA provide reliable and accurate *in vivo* markers for dynamic observations of pharmacokinetics and their interactions with cells.<sup>53</sup> Europium and terbium ion doping is based on their respective fluorescence properties. Under fluorescence irradiation, europium-doped ions show red fluorescence and terbium-doped ions show green fluorescence.<sup>54,55</sup> Magnesium ion doping modifies the morphology and physicochemical properties of nHA, improving the biological activity and reducing the crystallinity of the product by displacing some calcium ions. Anion dopants include chloride ions, fluoride ions, and carbonate ions, among others.<sup>56–58</sup> Chloride ions alter the morphology of nHA by partially displacing carbonate ions. After the substitution, crystal cell parameter *c* becomes

**Table 2. Comparing the Pros and Cons of Different Synthesis Methods for Synthetic Mg-nHA**

synthetic strategy	preponderance	disadvantage
hydrothermal synthesis	the synthesis method is simple and has few process control conditions	lattice defects are created, leading to an unstable crystal structure
hydrothermal synthesis–ion exchange	a simple way to prepare Mg-nHA particles with superior crystallinity, dispersion, and elevated purity	the rapid response speed led to an unmanageable size distribution and a diverse morphology of Mg-nHA particles
chemical precipitation	the morphology and average size of Mg-nHA particles were controllable	the low synthesis temperature can easily lead to the formation of other CaP phases, and multiple ions in the aqueous solution may enter the crystal structure and form impurities
mechanochemical synthesis	simple operation method, no process control requirements	experimental studies are less reported, and the test results are more biased
mechanochemical–hydrothermal synthesis	of the smaller nanoparticles, with good stability	Tval operation, many steps, process control indicators, easy to produce impurities
spark plasma sintering	time-consuming and simple process	the experimental equipment and environment necessitate stringent requirements, while also posing certain safety issues
biomimetic synthesis	low-temperature control, with a simple process	experimental studies have few reports and poor stability

**Figure 1.** A schematic representation of the emergence of synthesis methods for Mg-nHA.

smaller, parameters  $a$  and  $b$  become larger, lattice distortions and dilation occur, and the appearance changes from needle to sheet. The fluorine content changes the structure of fluorine-doped nHA and leads to changes in the chemical and biological properties.<sup>59</sup> As the fluorine content increases, the crystalline phase of the synthesized product changes appropriately, but the lattice parameters and the crystal plane spacing gradually decrease.<sup>60</sup> Carbonate doping is based on human solid tissue apatite, which contains varying levels of carbonate. nHA bioactivity can be increased by ion substitution.

### 3. SYNTHESIS OF NANOHYDROXYAPATITE

HA is a widely used biomaterial whose chemical structure and physical composition strongly affect its biological and mechanical properties *in vitro* and *in vivo*.<sup>61,62</sup> At present, researchers have adopted a variety of methods to prepare HA nanoparticles; however, most of the preparation methods are very limited in terms of economy and performance, and only a few synthetic methods can be applied to commercially or large-

scale synthesis.<sup>63</sup> These obstacles are not only the wide variety of surfactants, solvents, or precursor materials required in the synthesis process and stringent storage conditions but also the major agglomeration and phase impurities, the complex and costly processes, and the wide distribution of particle sizes.<sup>63</sup> Different preparation schemes have their advantages and disadvantages, as shown in Table 1. The preparation of nanoscale HA is varied. The usual strategy is to maximize size, crystallinity, particle agglomeration, stoichiometry, and geometry using synthesis methods that improve on existing processes and new routes.<sup>63–65</sup> It is now possible to synthesize nanoscale HA with specific compositions, repeatable sizes, and structures at large scales. In recent years, environmentally friendly fabrication methods,<sup>63</sup> including template synthesis, hydrothermal synthesis, molten salt synthesis, and biomimetics synthesis, have been widely recognized as viable techniques for a wide range of ceramic synthesis. nHA particles can be prepared by various drying process technologies, such as mechanical synthesis and solid-state fabrication. Ultrasound chemistry, microemulsions, polyols, hydrothermal synthesis,

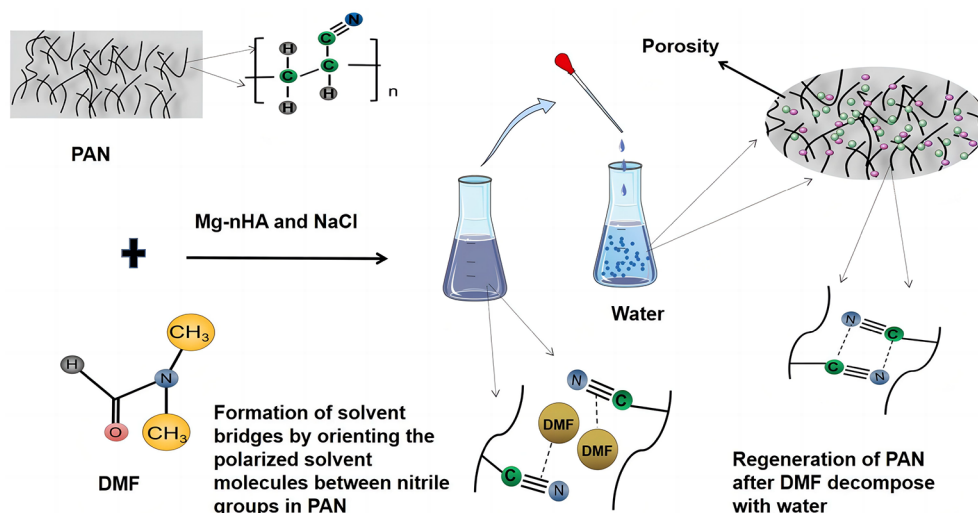


**Figure 2.** Schematic representation of the hybrid nanocomposite porous bead preparation process.

chemical coprecipitation, and sol–gel are other wet process technologies; high-temperature synthesis techniques such as thermal decomposition and combustion are also employed.

#### 4. SYNTHESIS METHOD OF MAGNESIUM-DOPED NANOHYDROXYAPATITE

Over the past 30 years, various methods have been reported for the preparation of nanoscale hydroxyapatite doped with magnesium ions, including Mg-nHA nanocrystalline whiskers and nanoparticles.<sup>90</sup> Since each preparation method has different control requirements on the device and the environment, it brings multiple submethods. Therefore, it is extremely difficult to employ specific submethods to prepare Mg-nHA under different experimental conditions, and the size and structure of the resulting nanoparticles are also different. From a literature review, we summarize the preparation methods. By comparing different methods (Table 2), a practical, economical and efficient scheme for obtaining Mg-nHA can be chosen. A schematic representation of the emergence of synthesis methods of magnesium-mixed nano-hydroxyapatite is shown in Figure 1.

**4.1. Mechanochemical–Hydrothermal Synthesis.** Mechanochemical–hydrothermal synthesis is a modified technique that combines mechanical methods with hydrothermal synthesis. Calcium salts, magnesium salts, and nitrates were dissolved in deionized water, vigorously stirred by a magnetic stirrer, and ground by grinding instruments to obtain initial Mg-nHA particles. The initial particles are treated with citrate at a certain temperature and pH to finally obtain purified particles. Specifically, first, 0–23.2 g of calcium hydroxide and 1.003–20 g of magnesium hydroxide powder were mixed with 350 mL of deionized water. Then, 25.892–29.41 g of ammonium hydrogen phosphate powder was added to the mixture under magnetic stirring for 10 min to maintain the molar ratio of (Ca + Mg)/P at 1.67. The pH of the mixture was controlled to be 9.94–10.44. The mixture was then put into a lab-scale mill equipped with a zirconia liner and the zirconia ring grinding medium for grinding. The treatment was started at 1500 rpm for 1 h at a temperature of 29 to 33 °C, followed by 800 rpm for 4 h at a temperature of 25–28 °C. The mixture was then centrifuged at 4500 rpm for 30 min, and the centrifuged precipitate was dried in an oven at 70 °C for 24

h and ground to a powder to obtain the prepared Mg-nHA. The prepared impure Mg-nHA powder containing unreacted magnesium hydroxide was then placed into a 0.2 M citric acid solution for purification. After solid-phase washing, the washed Mg-nHA powder was subsequently centrifuged at 4500 rpm for 30 min, dried in an oven at 70 °C for 24 h, and ground to a purified Mg-nHA powder.<sup>91</sup> Although this method can be used to prepare smaller nanoparticles, it is cumbersome with many steps, process control indicators, and easy impurity generation and has seen few applications in recent years.

Chen et al.<sup>92</sup> mixed  $(\text{Ca}(\text{OH})_2)$  and  $(\text{Mg}(\text{OH})_2)$  in deionized water and gradually added  $(\text{NH}_4)_2\text{HPO}_4$  to the mixed solution. The reaction mixture was stirred vigorously with a magnetic stirrer and a multiring medium mill with a rotation speed of 1000–5000 rpm at a reaction temperature of 22–32 °C. After freeze-drying, the initial particles were placed in an ammonium citrate bath solution, the final pH of which was adjusted to 8.9. The purified nanoparticles were obtained after a “citrate treatment” and a “heat treatment”. The freeze-dried powder was found to have a lower degree of agglomeration than regular oven-dried powder. The particle size can be reduced to 10.5 nm after treatment with pure citrate, and a large number of nanotubes can be produced repeatedly under controlled composition and phase conditions.

Suchanek et al.<sup>91</sup> also used  $\text{Ca}(\text{OH})_2$ ,  $\text{Mg}(\text{OH})_2$ , and  $(\text{NH}_4)_2\text{HPO}_4$  as raw materials. First, a suspension of a powder mixture containing  $\text{Ca}(\text{OH})_2$  and  $\text{Mg}(\text{OH})_2$  was prepared in deionized water in a glass beaker. Subsequently, the  $(\text{NH}_4)_2\text{HPO}_4$  powder was slowly added, and the slurry was placed in a laboratory-scale mill equipped with a zirconium liner and a zirconium ring grinding medium. High purity nanoparticles were obtained by purifying ammonium citrate water, and the stability of the particles was better after heat treatment at 900 °C. The concentration of Mg in Mg-nHA obtained by the mechanochemical–hydrothermal synthesis method is as high as 28.4 wt % compared to 5 wt % obtained by other methods of synthesizing Mg-nHA from aqueous solutions. The alternative level of Mg in Mg-nHA powder prepared by this preparation method is higher than those of nanoparticles prepared by other methods. As the number of Mg particles increases, the composites have higher osteoinductivity and other biological activity.

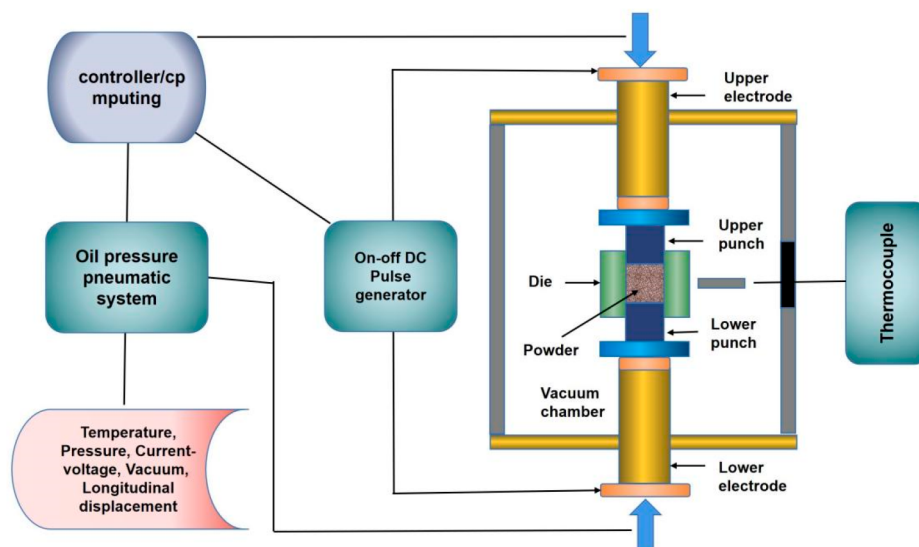


**Figure 3.** Schematic illustration of a spark plasma sintering (SPS) system for manufacturing magnesium–hydroxyapatite composites.

**4.2. Chemical Precipitation.** Among the many synthesis methods, chemical precipitation is one of the most widely used.<sup>14</sup> The advantage of chemical precipitation is that the morphology and average size of the product is controllable.<sup>93</sup> In the synthesis process, aqueous solutions of calcium salts and phosphates are mixed and then, after evaporation, sublimation, or hydrolysis, appropriate surfactants and pH regulators are chosen to gradually generate homogeneous Mg-nHA non-participants. Finally, the resulting precipitate is centrifuged, washed, and freeze-dried.<sup>94,95</sup> Concisely, 260 mL of solution containing 0.6 M calcium nitrate tetrahydrate and 0.2 M magnesium chloride hexahydrate were combined in 240 mL of 0.4 M ammonium dihydrophosphate solution (added to 4 M sodium hydroxide solution to maintain pH 9) and stirred under magnetic stirring conditions for 2 h. The white precipitate was separated by filtration on Whatman No.1 filter paper and rinsed several times with plenty of ultrapure water. The precipitate was dried at 50 °C for 24 h to yield Mg-nHA nanoparticles.<sup>96</sup> The main disadvantages of the wetting method are that the low synthesis temperature can easily lead to the formation of other CaP phases, and the second is that multiple ions in the aqueous solution may enter the crystal structure and form impurities.<sup>93,97</sup>

Alagarsamy et al.<sup>96,98</sup> synthesized by a chemical precipitation method using  $\text{Ca}(\text{NO}_3)_2 \cdot 4\text{H}_2\text{O}$ ,  $\text{MgCl}_2 \cdot 6\text{H}_2\text{O}$ , and  $(\text{NH}_4)_2\text{H}_2\text{PO}_4$  as raw materials and NaOH as pH regulator at 50 °C. Nanoparticles synthesized in this way have a rod-like structure with an average size of 82.62 nm. Alagarsamy's related research process<sup>96</sup> is shown in Figure 2.

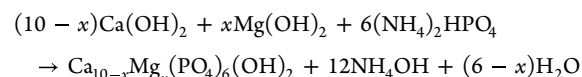
Using  $\text{Ca}(\text{NO}_3)_2 \cdot 4\text{H}_2\text{O}$ ,  $\text{MgCl}_2 \cdot 6\text{H}_2\text{O}$ , and  $(\text{NH}_4)_2\text{H}_2\text{PO}_4$  as raw materials and ammonia as the pH regulator, Shoba et al.<sup>94</sup> synthesized Mg-nHA by chemical precipitation at 90 °C. The nanoparticles synthesized in this way have a rod-like structure with an average size of 70 nm. It was also found that magnesium doping suppresses the crystallization of nanohydroxyapatite, resulting in smaller nanoparticles.

Lilley et al.<sup>99</sup> synthesized Mg-nHA by a chemical precipitation method using  $\text{Ca}(\text{NO}_3)_2 \cdot 4\text{H}_2\text{O}$ ,  $\text{Mg}(\text{NO}_3)_2 \cdot 6\text{H}_2\text{O}$ , and  $(\text{NH}_4)_2\text{H}_2\text{PO}_4$  as raw materials, ammonia as the pH regulator, pH = 11, and a controlled temperature of 25 °C. It has been found that the lattice parameters of nHA increase

with increasing magnesium content, which is thought to be due to the adsorption of magnesium onto the nHA core resulting in structural changes that destabilize the crystalline calcium phosphate. As the magnesium content increases, the mechanical properties of Mg-nHA decrease significantly.

**4.3. Mechanochemical Synthesis.** Mechanochemical synthesis<sup>100</sup> is a dry preparation technique in which calcium salt, phosphate, and magnesium salt powders are mixed in air and ground in a specific grinding apparatus according to a certain ratio of materials. The method is simple to operate and has no stringent environmental requirements during the experimental process. However, there are few reports on the fabrication techniques of this method, and the experimental results are somewhat biased. In the future, more experiments are needed to verify the feasibility and superiority of the preparation scheme.

Briefly, precursors  $\text{Ca}(\text{OH})_2$ ,  $(\text{NH}_4)_2\text{H}_2\text{PO}_4$ , and  $\text{Mg}(\text{OH})_2$  were mixed in a planetary ball mill with zirconia vials and ball as grinding medium, and the molar ratio of  $(\text{Ca} + \text{Mg})/\text{P}$  was 1.67. The powder-to-ball mass ratio is fixed at 1:5. Set the speed and milling time to 370 rpm and 15 h, respectively. Each milling session lasts 45 min, with a 15 min pause, resulting in the final Mg-doped hydroxyapatite particles.<sup>101</sup> The reaction equation for Mg-doped hydroxyapatite in three precursors is given in the following equation:



where  $x = 0, 0.1, 0.3, 0.5$  is denoted as the  $\text{Mg}^{2+}$  molar concentration. The different peak resolutions and broadening of the synthesized powders are due to the intensity of the nHA peak in the XRD decreasing with increasing  $\text{Mg}^{2+}$  concentration. This trend is also consistent with the results of studies Caciotti et al.<sup>102</sup> using the precipitation technique and the mechanical hydrothermal method.

**4.4. Spark Plasma Sintering.** Spark plasma sintering is a method of sintering samples with pure magnesium and pure nanohydroxyapatite powder under appropriate pressure in a vacuum environment using pulsed DC current.<sup>103–105</sup> In detail, magnesium powder and nanohydroxyapatite with an average particle size of 180  $\mu\text{m}$  and purities of 99.5% and 95%,

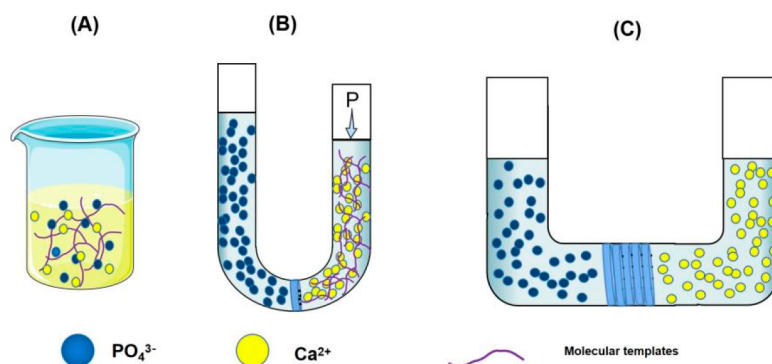


**Figure 4.** Process of fabricating apatite hybrid materials. (A) Coprecipitation method. The calcium solution is mixed with collagen and then a phosphate solution. (B) The collagen and calcium premixed solution is pressed through a filter membrane. The collagen fibers from the left side are mineralized when meeting phosphate solution. (C) The molecular templates are made into gels with porous structures. The calcium and phosphate ions diffuse into the gel and form crystals.

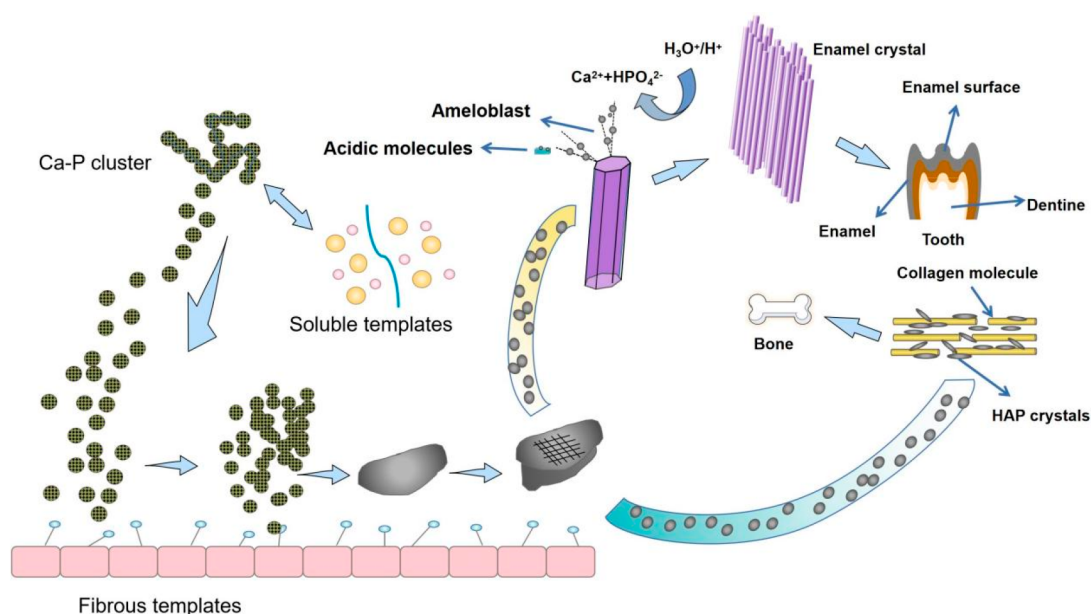


**Figure 5.** Mechanisms of the multimolecular template-regulated mineralization process by fibrous templates.

respectively, were used as starting powders. The two powders were mixed according to four combined forms (0, 8, 10, and 12 wt % HA, and the rest were Mg) in argon using a planetary microsphere mill at 500 rpm for 10 min. The different groups of mixed powders were then separately compacted at 10 MPa for 1 min to form a green powder in a graphite mold. Then, the cells were sintered by discharge plasma sintering (SPS) at 500 °C for 10 min under a uniaxial pressure of 50 MPa. Finally, Mg-doped nanohydroxyapatite was obtained. The preparation process is shown in Figure 3. Compared to conventional sintering methods, this technique has the advantages of high intensity, low voltage, and pulsed current and can sinter samples in a short time.<sup>106,107</sup> The powder is surrounded by a graphite mold and punch for compaction, and the copy paper is placed between the powder and punch for easy removal of the compaction after sintering. In the vacuum chamber, the graphite dies and the punch containing the powder are sandwiched between the graphite gaskets. Compared to conventional sintering methods, this method has a shorter sintering time and a smaller process.<sup>108,109</sup> After the sintering process, the samples were cooled to room temperature in a

vacuum chamber. However, this approach is highly demanding for experimental equipment and the experimental environment. The wide application of this synthesis method is limited by the fact that pure magnesium powder is prone to exploding in air, which introduces some security risks to the experiment. At the same time, the discharge and generation processes of plasma are highly controversial in the research community.<sup>110</sup>

Nakahata et al.<sup>110</sup> stirred the sample at 500 rpm for 10 min in an argon atmosphere using a planetary micro ball mill. The mixed powder is compacted in a graphite die for one min at 10 MPa to form a green compact. Then, spark plasma sintering (SPS) was performed at 500 °C and 50 MPa uniaxial pressure for ten min. Nanoparticles with a particle size of 32 nm were prepared. Although the process is performed under vacuum conditions, there is sufficient air between the powder in the chamber and the mold. Since the process is performed at high temperatures, oxidation occurs more readily than at room temperature. Therefore, this scheme is prone to impurities such as MgO.<sup>105,111</sup>

Moradi et al.<sup>112</sup> screened 800–900 μm pure magnesium particles and nanohydroxyapatite under the condition of a

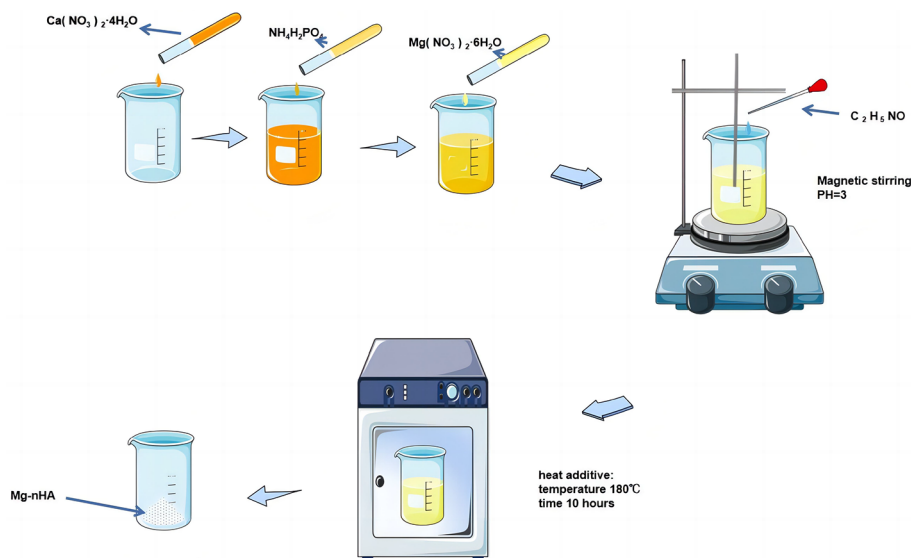


**Figure 6.** Experimental diagram of the preparation of Mg-nHA by hydrothermal synthesis.

spacer (urea) to prepare nanoparticles by plasma sintering. Experimental results show that the prepared nanoparticles are less than 30 nm in size and the nanoparticles of nano-hydroxyapatite are distributed almost uniformly over the magnesium matrix. Mechanical and corrosion tests showed that the Mg-nHA composites with 2 and 4 wt % had the best properties, with the same strength and elastic modulus as human cancellous bone.<sup>112,113</sup>

**4.5. Biomimetic Synthesis.** Mg-nHA materials were prepared by biomimetic mineralization, in which material ratios with a similar composition compared to human bone tissue are used to simulate the environmental growth and formation process of normal human bone tissue in an environment close to human temperature.<sup>114,115</sup> This method allows low temperatures to be controlled during preparation, and the process is simple and closer to the bone formation process. This is a highly effective preparative procedure that deserves further validation and improvement. First, 0.5 g of type I collagen was dissolved in 100 mL of deionized water, followed by the addition of 450 mL of 0.1 M calcium chloride, 50 mL of 0.1 M magnesium chloride, 300 mL of 0.1 M sodium hydrogen phosphate, 40 mL of 1 M citric acid, and 3.6 g of sodium chloride. The reaction took place in a water bath at 37 °C. After the mixture stirred for a period of time, a certain amount of 4 M sodium hydroxide solution was added dropwise, the pH was adjusted to 9–10, and the mixture was stirred for 2 h. Then, the obtained slurry was incubated in an incubator at 37 °C for 7 days. The resulting precipitate was suspended in 75% ethanol and centrifuged, and the washing process was repeated three times. Finally, the samples were freeze-dried to obtain Mg-nHA powder.<sup>92</sup> Ma et al.<sup>116,117</sup> prepared Mg-nHA nanoparticles by biomimetic mineralization using collagen fibers and citric acid as double template materials. The shape of the Mg-nHA particles is lamellar with a size of 30–50 nm, similar to the shape of HA in natural human bone. Ma's related research process<sup>117</sup> is shown in Figures 4 and 5.

However, the application of the experimental method in the preparation of Mg-nHA has rarely been reported, which makes the stability of this method in doubt. More relevant studies will be needed to confirm it later.

**4.6. Hydrothermal Synthesis.** Hydrothermal synthesis is the method of growing Mg-nHA at a certain pH, pressure, and temperature using aqueous solutions containing calcium, phosphorus, and magnesium as precursors and reacting solutions. After cooling, washing, and drying, the sample is ground into powdery nanoparticles. First, 0.1 mol/L  $\text{Ca}(\text{NO}_3)_2 \cdot 4\text{H}_2\text{O}$  solution, 0.06 mol/L  $\text{NH}_4\text{H}_2\text{PO}_4$  solution, and 0.1 mol/L  $\text{Mg}(\text{NO}_3)_2 \cdot 6\text{H}_2\text{O}$  solution were combined according to  $(\text{Ca} + \text{Mg})/\text{P} = 1.67$ . The solution of calcium ions, phosphate ions, and magnesium ions was mixed proportionally, and 1 mol/L acetamide solution was added as acid–base sustained-release agent. The solution was stirred evenly by a magnetic agitator, then the pH value of the solution was adjusted to 3. Finally, the prepared solution was put into a high-pressure reactor, the temperature was increased to 180 °C for reaction, and the target product Mg-nHA nanoparticles were obtained. The preparation process is shown in Figure 6.

The nHA prepared by Zhao et al.<sup>118</sup> by the hydrothermal method is hexagonal, and the average length and width of the particles are about 100 and 30 nm, respectively. The average length and width of Mg-nHA prepared in the same way are about 80 and 30 nm. The aspect ratio of the nanoparticles was found to decrease with increasing Mg content, which is thought to be caused by the suppression of grain growth and lattice distortion when the Mg element is substituted in nHA.<sup>118</sup> In the hydrothermal synthesis of Mg-nHA composite with an acid–base slow-release agent at pH = 3 and a temperature of 180 °C, Zhang et al.<sup>119</sup> found that with the increase of  $\text{Mg}^{2+}$  content. This is mainly because the radius of  $\text{Mg}^{2+}$  (70 pm) is smaller than that of  $\text{Ca}^{2+}$  (100 pm). When  $\text{Mg}^{2+}$  enters the nHA crystal to replace  $\text{Ca}^{2+}$ , lattice distortions are induced, directly leading to changes in the crystallinity, unit cell parameters, and morphology of nHA. When the doping of  $\text{Mg}^{2+}$  is less than 5%, the value of the unit cell parameter  $a$  of Mg-nHA remains essentially unchanged and the XRD shows no impurity phase. Only when the doping of  $\text{Mg}^{2+}$  reaches 8% does the value of  $a$  decrease, and the XRD pattern indicates the presence of an impurity phase, which is directly related to the difference in radii between the calcium and magnesium ions.<sup>119</sup> The rod-like Mg-nHA nanoparticles with uniform particle size,

a width of about 20 nm, a length of about 100 nm, and irregular pores of about 2–4 nm on the surface of the particles were obtained by hydrothermal synthesis using cetyltrimethylammonium bromide (CTAB) and ammonia solution ( $\text{NH}_3 \cdot \text{H}_2\text{O}$ ) as adjuvants. The obtained nanoparticles were found to be of high purity, and the Mg substitution had no effect on the morphology, particle size, zeta potential, or surface area of the nanoparticles.<sup>120</sup>

Hydrothermally synthesized nHA is typically a calcium-deficient apatite, and the phosphate in the crystal readily breaks down to form pyrophosphate upon heating. When  $\text{Mg}^{2+}$  enters the nHA lattice to replace  $\text{Ca}^{2+}$ , lattice defects are created, leading to an unstable crystal structure. In the nHA crystal containing calcium defects, the combination of  $\text{OH}^-$  is unstable and reacts with pyrophosphate to form the crystal phase of  $\beta$ -TCP. Therefore, the greater the concentration of  $\text{Mg}^{2+}$ , the more lattice defects, and the greater the content of  $\beta$ -TCP. When the calcination temperature gradually increases from 800 to 1000 °C, XDR shows additional impurity phases, indicating that the calcination temperature and the doping amount of  $\text{Mg}^{2+}$  are major technical difficulties affecting the nanosynthesis.<sup>119</sup>

**4.7. Hydrothermal Synthesis–Ion Exchange.** The hydrothermal synthesis–ion exchange method is a method to prepare Mg-nHA by hydrothermally synthesizing nHA, dispersing it into a solution containing  $\text{Mg}^{2+}$  particles, inducing cation exchange on the surface of the nanoparticle by magnetic stirring for a certain time, and finally washing, freezing, and drying. Briefly, a 60 mL solution containing 20 mM calcium nitrate tetrahydrate and 12 mM ammonia hydrogen phosphate was magnetically stirred and adjusted to a pH < 5 by adding nitric acid. Then, 0.9 g of sodium citrate triethyl dihydrate was added to the solution, and the mixture was transferred to the autoclave for another 15 min. After heating at 180 °C for 2 min, the nanohydroxyapatite particles were obtained by cleaning with deionized water and freeze-drying for 24 h. Then, 500 mg of nanohydroxyapatite particles were weighed and added into 50 mL of magnesium chloride solution, and the cationic exchange process was induced on the surface by magnetic stirring at room temperature for 24 h. The synthesized Mg-nHA particles were separated by ultracentrifugation (100 000 rpm, 15 min), washed with deionized water, freeze-dried for 24 h, and then collected by using a mortar and pestle.<sup>121</sup>

Mg-nHA and nHA show the same spectrum, indicating that the bulk structure of nHA does not change significantly after substitution. It moves to higher angles as the concentration of the  $\text{Mg}^{2+}$  solution increases. These results suggest that the substitution of  $\text{Mg}^{2+}$  on the bare nHA surface affects the lattice contraction along the *c*-axis direction. Cox et al.'s<sup>122–124</sup> description of the lattice change when  $\text{Mg}^{2+}$  is added to the HA structure is consistent.

It was confirmed that the substitution process introduces  $\text{Mg}^{2+}$  into the surface structure of nHA, which reduces the *c*-axis lattice parameter of nHA. In general, substitution by cations larger than  $\text{Ca}^{2+}$  leads to a lattice expansion of nHA, whereas substitution by smaller cations reduces the volume of *c*-axis dimensionally.<sup>125,126</sup>

Compared with other methods, this method is considered as a simple way to prepare Mg-nHA particles with superior crystallinity, dispersion, and elevated purity. However, the addition of a pH regulator shifts the pH value of the solution rapidly, resulting in extremely fast reaction rates. Therefore,

controlling the particle size distribution and morphology of Mg-nHA has become a major obstacle to the hydrothermal approach.

## 5. APPLICATIONS OF MAGNESIUM-DOPED NANOHYDROXYAPATITE

Magnesium-doped nanohydroxyapatite-based biomaterials have been reported in the field of biomedicine, mainly focusing on tissue engineering. In addition, there are a few reports in other fields such as bone defects, cartilage repair, periodontal diseases, angiogenesis, and cell transmembrane transmission.

The main goal of bone tissue engineering is to promote the integration and expedite the regeneration process of damaged bones. However, researchers have focused extensively on biodegradable polymer scaffolds due to various challenges associated with metal implants, such as stress shielding, palpation concerns, and worries about biocompatibility. Incorporating magnesium nanohydroxyapatite into these polymeric scaffolds not only enhances physical and chemical properties but also improves their biological characteristics and antibacterial activity. Lett et al.<sup>127</sup> utilized 3D printing to create a scaffold made of Mg-doped hydroxyapatite-coated polylactic acid (PLA). The synthesized composite exhibited a three-dimensional porous structure and demonstrated excellent blood compatibility, thereby facilitating efficient nutrient delivery and promoting protein uptake. Magnesium-doped nanohydroxyapatite scaffolds based on PLA were synthesized by Swetha et al.<sup>128</sup> and demonstrated exceptional cell adhesion properties and verified osteogenic potential at the cellular level through mesenchymal stem cells assay. Sedghi et al.<sup>129</sup> successfully grafted polycaprolactone onto chitosan and developed a novel scaffold based on copper(I)-catalyzed azido-alkynyl cycloaddition (CuAAC), incorporating Mg-nHA. Their findings demonstrated that the incorporation of a triazole ring into the copolymer chemical structure significantly enhanced the bone mineralization ability of the fabricated scaffold while exhibiting negligible cytotoxicity. The effect of incorporating zinc ions into magnesium-doped nanohydroxyapatite-based biomaterials remains controversial. Kazimierzak et al.<sup>130</sup> investigated the addition of magnesium and zinc ions to chitosan–agarose–hydroxyapatite scaffolds but did not observe any enhancement in biological properties compared to the sole addition of zinc ions. They proposed that including zinc ions in polymer scaffolds based on Mg-doped nanohydroxyapatite did not yield favorable effects on cellular behavior. Conversely, Dittler et al.<sup>131</sup> arrived at an opposing conclusion, potentially due to variances in experimental outcomes arising from disparate scaffold materials employed by both groups. Consequently, further experiments are needed to validate the biological performance. Furthermore, Scalera et al.<sup>132</sup> successfully fabricated nanoporous scaffolds made from magnesium-doped Sr-limestone using high-temperature sintering to achieve exceptional thermal stability. According to their findings, the presence of 0.5 wt % magnesium and strontium leads to optimal thermal stability and mechanical properties, emphasizing the essential role of Mg and Sr doping in attaining bone remodeling functionality in a promising bone-mimetic matrix suitable for cellular growth and proliferation.

In the investigation of bone defect repair, Ahmadzadeh et al.<sup>133</sup> conducted a study in which they implanted Mg-nHA particles in a rabbit tibial osteotomy model and evaluated the ability of the graft to promote bone tissue growth in vivo.

Upon examination 4fourweeks after surgery, the grafts were successfully replaced by new calcified tissue without any signs of inflammation or infection. Therefore, it can be concluded that grafts constructed with Mg-doped nanohydroxyapatite are an effective alternative material for conductive bone tissue.

In the study of a biocoating application, Xing et al.<sup>134</sup> used nHA derived from porcine bone to synthesize magnesium-doped particles, which were then coated onto the surface of porcine bone. The results of both in vivo and in vitro experiments showed that 20% Mg-doped nHA displayed superior osteogenic properties and effectively eliminated excess material while maintaining an inherent average pore size of 300  $\mu\text{m}$ , a three-dimensional porous skeleton structure, and controlled release of magnesium ions with immunomodulatory effects on macrophages at appropriate concentrations.

In the past few years, researchers have been primarily focused on finding solutions to the difficulties related to the regeneration of bone and cartilage. Chitosan has emerged as a highly regarded biomaterial in this field due to its exceptional ability to enhance both cartilage and bone healing. Roffi et al.<sup>135</sup> developed a novel composite scaffold incorporating magnesium-doped hydroxyapatite and assessed its potential for bone-cartilage regeneration in a sheep model to investigate the regenerative capacity of collagen and chitosan scaffolds. However, their study did not observe any discernible regeneration of cartilage or the underlying bone tissue. These findings suggest that further research is required to determine the optimal formulation of magnesium-doped hydroxyapatite-enhanced composite materials for applications in bone-cartilage regeneration.

Typically, tooth extraction or periodontal disease can have an impact on the supporting tissues surrounding the teeth, including the periodontal ligament, alveolar tissue, and gingival tissue. The objective of periodontal treatment is to promote cell regeneration through a concept of tissue regeneration. However, in clinical practice, secondary surgery becomes necessary due to the nondegradability of most biomaterials. Introducing a biodegradable nanofiber scaffold made from polymers for delivering essential regenerative bioactive substances represents a relatively novel approach. Shoba et al.<sup>94</sup> discovered that incorporating Mg-nHA into a functionalized polymer scaffold significantly enhances its biological, thermal, physicochemical, and mechanical properties. Moreover, the synthesized nanobiomaterial exhibits promising antibacterial activity and blood compatibility and also improves the cell proliferation capability and the migration rate in in vitro experiments. Canullo et al.<sup>136</sup> conducted a clinical trial to observe patients who had undergone ridge preservation surgery for either 4 or 12 months. They found that at the 4 month mark, collagen matrix remodeling started from the apex and proceeded in a coronal direction, showing increased activity around the transplanted particles. After 12 months following surgery, complete socket regeneration was observed, with well-structured mineralized bone tissue filling in around the remaining biomaterial particles. These findings also verified substantial degradation and absorption of the transplanted material throughout the experimental period. Based on the aforementioned fundamental and clinical trials, it can be inferred that biomaterials based on Mg-nHA exhibit significant potential for advancement in the field of oral medicine.

Despite the substantial influence of ion substitution on the biological performance of hydroxyapatite, there is still a limited understanding regarding its effects on nanoparticles. Several

researchers have examined the microscopic perspective to explore how cellular behavior is influenced by Mg-nHA. Bonany et al.<sup>137</sup> employed two distinct types of nanoparticles, nHA and Mg-nHA, to investigate their interaction with MG-63 cells. Following the introduction of these nanoparticles during cell culture, the authors observed the formation of numerous calcium-rich vesicles through calcium fluorescence probe imaging. These multivesicular bodies potentially serve as reservoirs for calcium ions upon cellular uptake. Furthermore, it was confirmed at a microscopic level that these nanoparticles undergo significant degradation within MG-63 cells, thus validating the biodegradable properties of Mg-nHA. The theory of nanoparticle internalization still presents several unresolved issues; however, it has also revealed numerous novel possibilities. In their investigation on the impact of magnesium-doped hydroxyapatite nanoparticles on cellular behavior, Zhao et al.<sup>138</sup> made a significant observation that the surface charge of nanoparticles profoundly influences MG-63 cells. Excessive negative charge hinders internalization; nevertheless, this phenomenon was not observed in experiments involving bone marrow mesenchymal stem cells. Consequently, we can conclude that magnesium doping primarily affects MG-63 cells with high cytotoxicity and does not exert any influence on bone marrow mesenchymal stem cells. This finding further substantiates the notion that stimulants can serve as valuable tools for modulating nanoparticle internalization.

However, it is worth mentioning that a limited number of papers have conducted comprehensive evaluations on the in vivo biological characteristics of biomaterials based on Mg-nHA. Despite many in vivo studies carried out and published on these materials, their outcomes often fail to meet the criteria for large-scale production. Bridging the divide between laboratory research and clinical implementation will necessitate substantial endeavors. It is crucial to establish close collaboration among chemists, scientists, biologists, bioengineers, and clinicians in order to transform intriguing research discoveries into medically applicable materials.

## 6. CONCLUSION AND FUTURE PROSPECTS

This Perspective mainly introduces the preparation techniques of various Mg-nHAs. The physicochemical properties of nanoparticles are often affected by the morphology and crystallinity of the particles. We found that the particle synthesis process played an important role in the formation of the morphology and crystallinity of the Mg-doped nanoparticles. Different morphologies of Mg-nHA particles (rod-like, flake-like, and rod-like) can be prepared due to different precursors, pH levels, temperature, pressure, etc.

The Mg-nHA particles prepared by hydrothermal synthesis have a rod-like structure, and the particle size is less than 100 nm. When the amount of  $\text{Mg}^{2+}$  is not more than 5 wt %, the obtained nanoparticles have high purity, and Mg substitution has no effect on the morphology, particle size, zeta potential, and surface area of the nanoparticles. The hydrothermal synthesis ion exchange method is regarded as a simple method for preparing samples with crystallinity, high purity, and good dispersion. The obtained Mg-nHA particles exhibit no obvious change in the shape and structure of the original nanohydroxyapatite particles. The disadvantage of this preparatory approach is that the addition of pH regulator in the synthesis process makes the pH value of the solution change rapidly, resulting in a too fast reaction rate and affecting the particle

size distribution and morphology of the nanoparticles. Chemical precipitation is one of the most widely used methods. This method can prepare Mg-nHA particles with controllable morphology and uniform particles at low temperature. It is also these low temperature conditions that are more likely to cause the formation of CP phase impurities during the synthesis. As a dry synthesis technology, mechanochemical synthesis is simple to operate and has no stringent environmental requirements during the experimental process. This is the most suitable and most worthy preparation strategy, but there are few reports on this method in the past decade, and the validity and reliability of the results are questioned. Mechanochemical–hydrothermal synthesis is an innovative synthesis scheme. Combining the advantages of mechanochemical and hydrothermal synthesis, Mg-nHA with a smaller particle size (10.5 nm) can be prepared and can be repeatedly produced under the condition of controlling composition and phase. The combination of the two methods increases the complexity of the preparation process and the difficulty of process control, and the purity of the obtained product is also challenged. The spark plasma sintering method is used to synthesize Mg-nHA particles under a vacuum environment in high-temperature and high-pressure conditions. The synthesized particles have a small particle size (<30 nm) and uniform distribution. Due to the high requirements for the experimental process and experimental equipment, the wide promotion of this preparation method is extremely limited. Biomimetic mineralization is one of the various preparation methods. The preparation environment, conditions, and precursors are closest to the growth and formation process of real human bone tissue. This is an ideal method of synthesis and deserves extensive study and generalization.

To date, there are still many open questions and challenges within this field that need to be investigated in detail. Future trends in the morphology and properties of Mg-nHA for biomedical applications may lie in the following areas: (1) The application of Mg-nHA is still in its infancy, and further research is needed, such as whether Mg-nHA can significantly improve biocompatibility and bone induction in artificial biomaterials. (2) A key question to be addressed is the lattice defects of the Mg-nHA particles. Effective strategies to reduce lattice defects in experimental products should be further investigated in future experimental studies. (3) There have been many studies on the morphological control of nanoparticles during preparation but very few on the fine-size control. Understanding the reaction mechanisms of a different method of synthesis will not only help to improve existing techniques but may also shed new light on the development of new control strategies to obtain nanoparticles with better morphology and size. (4) Although various methods have been reported for preparing Mg-nHA, the resulting nanoparticles vary widely in size. The synthesis of stable, homogeneous, high-aspect-ratio Mg-nHA will be a hot topic in the future.

## AUTHOR INFORMATION

### Corresponding Author

Wenji Wang – Department of Orthopedics, The First Hospital of Lanzhou University, Lanzhou, Gansu 730000, China; Phone: +8613893221698; Email: [ldyyjzwwj@outlook.com](mailto:ldyyjzwwj@outlook.com)

## Authors

Kui Zhang – The First Clinical Medical College of Lanzhou University, Lanzhou, Gansu 730000, China; [orcid.org/0009-0004-8844-7217](https://orcid.org/0009-0004-8844-7217)

Yan Liu – Department of Gynecology, First Affiliated Hospital of Xi'an Medical College, Xi'an, Shaanxi 710000, China

Zhenrui Zhao – The First Clinical Medical College of Lanzhou University, Lanzhou, Gansu 730000, China

Xuewen Shi – The First Clinical Medical College of Lanzhou University, Lanzhou, Gansu 730000, China

Ruihao Zhang – The First Clinical Medical College of Lanzhou University, Lanzhou, Gansu 730000, China

Yixiang He – The First Clinical Medical College of Lanzhou University, Lanzhou, Gansu 730000, China

Huaibin Zhang – The First Clinical Medical College of Lanzhou University, Lanzhou, Gansu 730000, China

Yi Sun – The First Clinical Medical College of Lanzhou University, Lanzhou, Gansu 730000, China

Complete contact information is available at:

<https://pubs.acs.org/10.1021/acsomega.3c06091>

## Author Contributions

These authors contributed equally: Kui Zhang and Yan Liu.

## Notes

The authors declare no competing financial interest.

## ACKNOWLEDGMENTS

We thank the Lanzhou University Library for providing a free retrieval database platform for this manuscript.

## REFERENCES

- (1) Qu, H.; Fu, H.; Han, Z.; Sun, Y. Biomaterials for bone tissue engineering scaffolds: a review. *RSC Adv.* **2019**, *9* (45), 26252–26262.
- (2) Hou, X.; Zhang, L.; Zhou, Z.; Luo, X.; Wang, T.; Zhao, X.; Lu, B.; Chen, F.; Zheng, L. Calcium Phosphate-Based Biomaterials for Bone Repair. *Journal of Functional Biomaterials* **2022**, *13* (4), 187.
- (3) Zhang, X.; Li, Q.; Wang, Z.; Zhou, W.; Zhang, L.; Liu, Y.; Xu, Z.; Li, Z.; Zhu, C.; Zhang, X. Bone regeneration materials and their application over 20 years: A bibliometric study and systematic review. *Front Bioeng Biotechnol* **2022**, *10*, 921092.
- (4) Mudhafar, M.; Alsailawi, H.; Raheem, H. A.; Mohammed, R. K. A REVIEW STUDY ON THE BIOMATERIALS AND BONE GRAFTS FOR BONE DEFECTS APPLICATIONS. *Eur. J. Biomed.* **2022**, *9* (4), 63–73.
- (5) Qu, X.; Yang, H.; Yu, Z.; Jia, B.; Qiao, H.; Zheng, Y.; Dai, K. Serum zinc levels and multiple health outcomes: Implications for zinc-based biomaterials. *Bioactive Materials* **2020**, *5* (2), 410–422.
- (6) Henkel, J.; Woodruff, M. A.; Epari, D. R.; Steck, R.; Glatt, V.; Dickinson, I. C.; Choong, P. F.; Schuetz, M. A.; Hutmacher, D. W. Bone regeneration based on tissue engineering conceptions—A 21st century perspective. *Bone research* **2013**, *1* (1), 216–248.
- (7) Kumar, S.; Nehra, M.; Kedia, D.; Dilbaghi, N.; Tankeshwar, K.; Kim, K.-H. Nanotechnology-based biomaterials for orthopaedic applications: Recent advances and future prospects. *Materials science and engineering: C* **2020**, *106*, 110154.
- (8) Zhu, L.; Luo, D.; Liu, Y. Effect of the nano/microscale structure of biomaterial scaffolds on bone regeneration. *Int. J. Oral. Sci.* **2020**, *12*, 6.
- (9) Pina, S.; Oliveira, J. M.; Reis, R. L. Natural-based nanocomposites for bone tissue engineering and regenerative medicine: A review. *Adv. Mater.* **2015**, *27* (7), 1143–1169.
- (10) Shi, H.; Zhou, Z.; Li, W.; Fan, Y.; Li, Z.; Wei, J. Hydroxyapatite based materials for bone tissue engineering: A brief and comprehensive introduction. *Crystals* **2021**, *11* (2), 149.

- (11) Predoi, D.; Iconaru, S. L.; Predoi, M. V.; Stan, G. E.; Buton, N. Synthesis, characterization, and antimicrobial activity of magnesium-doped hydroxyapatite suspensions. *Nanomaterials (Basel)* **2019**, *9* (9), 1295.
- (12) Raafat, A. I.; Kamal, H.; Sharada, H. M.; Abd Elhalim, S. A.; Mohamed, R. D. Radiation synthesis of magnesium doped nano hydroxyapatite/(acacia-gelatin) scaffold for bone tissue regeneration: in vitro drug release study. *Journal of Inorganic and Organometallic Polymers and Materials* **2020**, *30*, 2890–2906.
- (13) Kazakova, G.; Safronova, T.; Golubchikov, D.; Shevtsova, O.; Rau, J. V. Resorbable Mg<sup>2+</sup>-containing phosphates for bone tissue repair. *Materials* **2021**, *14* (17), 4857.
- (14) Jenifer, A.; Senthilarasan, K.; Arumugam, S.; Sivaprakash, P.; Sagadevan, S.; Sakthivel, P. Investigation on antibacterial and hemolytic properties of magnesium-doped hydroxyapatite nano-composite. *Chem. Phys. Lett.* **2021**, *771*, 138539.
- (15) Stipnice, L.; Salma-Ancane, K.; Borodajenko, N.; Sokolova, M.; Jakovlevs, D.; Berzina-Cimdina, L. Characterization of Mg-substituted hydroxyapatite synthesized by wet chemical method. *Ceram. Int.* **2014**, *40* (2), 3261–3267.
- (16) Wang, L.-L.; Liu, X.-X.; Zhou, Y.-M.; Wang, X.-F. Preparation of ordered porous Mg-HA and drug sustained-release performance. *Materials and Manufacturing Processes* **2022**, *37* (13), 1500–1505.
- (17) Pazarlioglu, S.; Algan, O.; Isikogullari, M. A.; Gokce, H. The effect of lanthanum addition on the microstructure and mechanical properties of Mg-modified hydroxyapatite ceramics. *Processing and Application of Ceramics* **2021**, *15* (3), 226–237.
- (18) Sun, Y.; Yuan, K.; Lou, J.; Yu, J.; Yu, H.; Peng, Z.; Dong, X.; Hou, P.; Zan, R.; Peng, H.; et al. Particles Generated from Degrading Magnesium Implants Induce Bone Resorption. *Research Square* **2022**, DOI: 10.21203/rs.3.rs-2093365/v1.
- (19) Al-Fartusie, F. S.; Mohssan, S. N. Essential trace elements and their vital roles in human body. *Indian J. Adv. Chem. Sci.* **2017**, *5* (3), 127–136.
- (20) Dermience, M.; Lognay, G.; Mathieu, F.; Goyens, P. Effects of thirty elements on bone metabolism. *Journal of Trace Elements in Medicine and Biology* **2015**, *32*, 86–106.
- (21) Bairagi, D.; Mandal, S. A comprehensive review on biocompatible Mg-based alloys as temporary orthopaedic implants: Current status, challenges, and future prospects. *Journal of Magnesium and Alloys* **2022**, *10* (3), 627–669.
- (22) Tan, J.; Ramakrishna, S. Applications of magnesium and its alloys: A review. *Applied Sciences* **2021**, *11* (15), 6861.
- (23) Wang, J. L.; Xu, J. K.; Hopkins, C.; Chow, D. H. K.; Qin, L. Biodegradable magnesium-based implants in orthopedics—a general review and perspectives. *Adv. Sci.* **2020**, *7* (8), 1902443.
- (24) Istrate, B.; Munteanu, C.; Antoniac, I.-V.; Lupescu, Ș.-C. Current Research Studies of Mg-Ca-Zn Biodegradable Alloys Used as Orthopedic Implants. *Crystals* **2022**, *12* (10), 1468.
- (25) Poinern, G. E. J.; Brundavanam, S.; Fawcett, D. Biomedical magnesium alloys: a review of material properties, surface modifications and potential as a biodegradable orthopaedic implant. *Am. J. Biomed. Eng.* **2012**, *2* (6), 218–240.
- (26) Zhao, D.; Witte, F.; Lu, F.; Wang, J.; Li, J.; Qin, L. Current status on clinical applications of magnesium-based orthopaedic implants: A review from clinical translational perspective. *Biomaterials* **2017**, *112*, 287–302.
- (27) Amukarimi, S.; Mozafari, M. Biodegradable magnesium-based biomaterials: An overview of challenges and opportunities. *MedComm* **2021**, *2* (2), 123–144.
- (28) Zhou, H.; Liang, B.; Jiang, H.; Deng, Z.; Yu, K. Magnesium-based biomaterials as emerging agents for bone repair and regeneration: from mechanism to application. *Journal of Magnesium and Alloys* **2021**, *9* (3), 779–804.
- (29) Witte, F. The history of biodegradable magnesium implants: a review. *Acta Biomaterialia* **2010**, *6* (5), 1680–1692.
- (30) Seal, C.; Vince, K.; Hodgson, M. Biodegradable surgical implants based on magnesium alloys—A review of current research. *IOP Conf. Ser.: Mater. Sci. Eng.* **2009**, *4*, 012011 DOI: 10.1088/1757-899X/4/1/012011.
- (31) Hiromoto, S.; Yamamoto, A. High corrosion resistance of magnesium coated with hydroxyapatite directly synthesized in an aqueous solution. *Electrochim. Acta* **2009**, *54* (27), 7085–7093.
- (32) Yao, W.; Liang, W.; Huang, G.; Jiang, B.; Atrons, A.; Pan, F. Superhydrophobic coatings for corrosion protection of magnesium alloys. *Journal of Materials Science & Technology* **2020**, *52*, 100–118.
- (33) Yin, X.; Mu, P.; Wang, Q.; Li, J. Superhydrophobic ZIF-8-based dual-layer coating for enhanced corrosion protection of Mg alloy. *ACS Appl. Mater. Interfaces* **2020**, *12* (31), 35453–35463.
- (34) Sezer, N.; Evis, Z.; Kayhan, S. M.; Tahmasebifar, A.; Koç, M. Review of magnesium-based biomaterials and their applications. *Journal of magnesium and alloys* **2018**, *6* (1), 23–43.
- (35) Jing, X.; Ding, Q.; Wu, Q.; Su, W.; Yu, K.; Su, Y.; Ye, B.; Gao, Q.; Sun, T.; Guo, X. Magnesium-based materials in orthopaedics: material properties and animal models. *Biomater. Transl.* **2021**, *2* (3), 197–213.
- (36) Gu, X.-N.; Zheng, Y.-F. A review on magnesium alloys as biodegradable materials. *Frontiers of Materials Science in China* **2010**, *4* (2), 111.
- (37) Grün, N. G.; Holweg, P.; Tangl, S.; Eichler, J.; Berger, L.; Van den Beucken, J. J.; Löffler, J. F.; Klestil, T.; Weinberg, A. M. Comparison of a resorbable magnesium implant in small and large growing-animal models. *Acta Biomaterialia* **2018**, *78*, 378–386.
- (38) Wang, J.; Witte, F.; Xi, T.; Zheng, Y.; Yang, K.; Yang, Y.; Zhao, D.; Meng, J.; Li, Y.; Li, W.; et al. Recommendation for modifying current cytotoxicity testing standards for biodegradable magnesium-based materials. *Acta Biomater.* **2015**, *21*, 237–249.
- (39) Pogorielov, M.; Husak, E.; Solodivnik, A.; Zhdanov, S. Magnesium-based biodegradable alloys: Degradation, application, and alloying elements. *Interventional Medicine and Applied Science* **2017**, *9* (1), 27–38.
- (40) Uppal, G.; Thakur, A.; Chauhan, A.; Bala, S. Magnesium based implants for functional bone tissue regeneration—A review. *Journal of Magnesium and Alloys* **2022**, *10* (2), 356–386.
- (41) Du, M.; Chen, J.; Liu, K.; Xing, H.; Song, C. Recent advances in biomedical engineering of nano-hydroxyapatite including dentistry, cancer treatment and bone repair. *Composites Part B: Engineering* **2021**, *215*, 108790.
- (42) Zhou, H.; Lee, J. Nanoscale hydroxyapatite particles for bone tissue engineering. *Acta Biomaterialia* **2011**, *7* (7), 2769–2781.
- (43) Venkatesan, J.; Kim, S.-K. Nano-hydroxyapatite composite biomaterials for bone tissue engineering—a review. *Journal of biomedical nanotechnology* **2014**, *10* (10), 3124–3140.
- (44) Abere, D. V.; Ojo, S. A.; Oyatogun, G. M.; Paredes-Epinosa, M. B.; Niluxshun, M. C. D.; Hakami, A. Mechanical and morphological characterization of nano-hydroxyapatite (nHA) for bone regeneration: A mini review. *Biomedical Engineering Advances* **2022**, *4*, 100056.
- (45) Ielo, I.; Calabrese, G.; De Luca, G.; Conoci, S. Recent advances in hydroxyapatite-based biocomposites for bone tissue regeneration in orthopedics. *International Journal of Molecular Sciences* **2022**, *23* (17), 9721.
- (46) Asadniaey Fardjahromi, M.; Nazari, H.; Ahmadi Tafti, S. M.; Razmjou, A.; Mukhopadhyay, S.; Warkiani, M. E. Metal-organic framework-based nanomaterials for bone tissue engineering and wound healing. *Materials Today Chemistry* **2022**, *23*, 100670.
- (47) Sindoro, M.; Yanai, N.; Jee, A. Y.; Granick, S. Colloidal-sized metal-organic frameworks: synthesis and applications. *Acc. Chem. Res.* **2014**, *47* (2), 459–69.
- (48) Shyngys, M.; Ren, J.; Liang, X.; Miao, J.; Blocki, A.; Beyer, S. Metal-Organic Framework (MOF)-Based Biomaterials for Tissue Engineering and Regenerative Medicine. *Front Bioeng Biotechnol* **2021**, *9*, 603608.
- (49) Sengar, P.; Chauhan, K.; Hirata, G. A. Progress on carbon dots and hydroxyapatite based biocompatible luminescent nanomaterials for cancer theranostics. *Translational Oncology* **2022**, *24*, 101482.

- (50) Wieszczycka, K.; Staszak, K.; Woźniak-Budych, M. J.; Jurga, S. Lanthanides and tissue engineering strategies for bone regeneration. *Coord. Chem. Rev.* **2019**, *388*, 248–267.
- (51) Schatkoski, V. M.; do Amaral Montanheiro, T. L.; de Menezes, B. R. C.; Pereira, R. M.; Rodrigues, K. F.; Ribas, R. G.; da Silva, D. M.; Thim, G. P. Current advances concerning the most cited metal ions doped bioceramics and silicate-based bioactive glasses for bone tissue engineering. *Ceram. Int.* **2021**, *47* (3), 2999–3012.
- (52) Song, T.; Zhao, F.; Wang, Y.; Li, D.; Lei, N.; Li, X.; Xiao, Y.; Zhang, X. Constructing a biomimetic nanocomposite with the in situ deposition of spherical hydroxyapatite nanoparticles to induce bone regeneration. *J. Mater. Chem. B* **2021**, *9* (10), 2469–2482.
- (53) Qiao, H.; Song, G.; Huang, Y.; Yang, H.; Han, S.; Zhang, X.; Wang, Z.; Ma, J.; Bu, X.; Fu, L. Si, Sr, Ag co-doped hydroxyapatite/TiO<sub>2</sub> coating: enhancement of its antibacterial activity and osteoinductivity. *RSC Adv.* **2019**, *9* (24), 13348–13364.
- (54) Neacsu, I. A.; Stoica, A. E.; Vasile, B. S.; Andronesu, E. Luminescent hydroxyapatite doped with rare earth elements for biomedical applications. *Nanomaterials (Basel)* **2019**, *9* (2), 239.
- (55) Perera, T. S. H.; Han, Y.; Lu, X.; Wang, X.; Dai, H.; Li, S. Rare earth doped apatite nanomaterials for biological application. *J. Nanomater.* **2015**, *2015*, 705390.
- (56) Panda, S.; Biswas, C. K.; Paul, S. A comprehensive review on the preparation and application of calcium hydroxyapatite: A special focus on atomic doping methods for bone tissue engineering. *Ceram. Int.* **2021**, *47* (20), 28122–28144.
- (57) Cacciotti, I. Multisubstituted hydroxyapatite powders and coatings: The influence of the codoping on the hydroxyapatite performances. *International Journal of Applied Ceramic Technology* **2019**, *16* (5), 1864–1884.
- (58) Bhat, S.; Uthappa, U.; Altalhi, T.; Jung, H.-Y.; Kurkuri, M. D. Functionalized porous hydroxyapatite scaffolds for tissue engineering applications: a focused review. *ACS Biomaterials Science & Engineering* **2022**, *8* (10), 4039–4076.
- (59) Karamian, E.; Abdellahi, M.; Khandan, A.; Abdellah, S. Introducing the fluorine doped natural hydroxyapatite-titania nano-biocomposite ceramic. *J. Alloys Compd.* **2016**, *679*, 375–383.
- (60) Fathi, M.; Zahrani, E. M. Mechanical alloying synthesis and bioactivity evaluation of nanocrystalline fluoridated hydroxyapatite. *J. Cryst. Growth* **2009**, *311* (5), 1392–1403.
- (61) Samavedi, S.; Whittington, A. R.; Goldstein, A. S. Calcium phosphate ceramics in bone tissue engineering: A review of properties and their influence on cell behavior. *Acta Biomaterialia* **2013**, *9* (9), 8037–8045.
- (62) Thirivikraman, G.; Madras, G.; Basu, B. In vitro/In vivo assessment and mechanisms of toxicity of bioceramic materials and its wear particulates. *RSC Adv.* **2014**, *4* (25), 12763–12781.
- (63) Mondal, S.; Dorozhkin, S. V.; Pal, U. Recent progress on fabrication and drug delivery applications of nanostructured hydroxyapatite. *WIREs Nanomed. Nanobiotechnol.* **2018**, *10* (4), No. e1504.
- (64) Rial, R.; González-Durruthy, M.; Liu, Z.; Ruso, J. M. Advanced Materials Based on Nanosized Hydroxyapatite. *Molecules* **2021**, *26* (11), 3190.
- (65) Sadat-Shojai, M.; Khorasani, M.-T.; Dinpanah-Khoshdargi, E.; Jamshidi, A. Synthesis methods for nanosized hydroxyapatite with diverse structures. *Acta Biomaterialia* **2013**, *9* (8), 7591–7621.
- (66) Joshi, K. J.; Shah, N. M. Study of Hydroxyapatite Nanoparticles synthesized using sono-chemical supported hydrothermal method. *Materials Today: Proceedings* **2021**, *47*, 505–509.
- (67) Poinern, G.; Rattan, S.; Brundavanam, R.; Fawcett, D.; Tennant, M.; Granich, J.; Burt, M., Improved Sono-chemical synthesis of hydroxyapatite nanorods as a dental restorer filler materials. *AU 2021106547 A4*, **2021**.
- (68) Manafi, S. A.; Joughehdoust, S. Synthesis of Hydroxyapatite Nanostructure by Hydrothermal Condition for Biomedical Application. *Iran. J. Pharm. Sci.* **2009**, *5* (2), 89–94.
- (69) Mechay, A.; Feki, H. E. L.; Schoenstein, F.; Jouini, N. Nanocrystalline hydroxyapatite ceramics prepared by hydrolysis in polyol medium. *Chem. Phys. Lett.* **2012**, *541*, 75–80.
- (70) Shih, W.-J.; Wang, M.-C.; Hon, M.-H. Morphology and crystallinity of the nanosized hydroxyapatite synthesized by hydrolysis using cetyltrimethylammonium bromide (CTAB) as a surfactant. *J. Cryst. Growth* **2005**, *275* (1–2), e2339–e2344.
- (71) Amin, S.; Siddique, T.; Mujahid, M.; Shah, S. S. Synthesis and Characterization of Nano Hydroxyapatite using Reverse Micro Emulsions as Nano Reactors. *J. Chem. Soc. Pak.* **2015**, *37* (1), 79–85.
- (72) Li, H.; Zhu, M.; Li, L.; Zhou, C. Processing of nanocrystalline hydroxyapatite particles via reverse microemulsions. *JOURNAL OF MATERIALS SCIENCE* **2008**, *43* (1), 384–389.
- (73) Neira, I. S.; Kolen'ko, Y. V.; Lebedev, O. I.; Van Tendeloo, G.; Gupta, H. S.; Guitian, F.; Yoshimura, M. An Effective Morphology Control of Hydroxyapatite Crystals via Hydrothermal Synthesis. *Cryst. Growth Des.* **2009**, *9* (1), 466–474.
- (74) Jokanovic, V.; Izvonar, D.; Dramicanin, M. D.; Jokanovic, B.; Zivojinovic, V.; Markovic, D.; Dacic, B. Hydrothermal synthesis and nanostructure of carbonated calcium hydroxyapatite. *Journal of Materials Science-Materials in Medicine* **2006**, *17* (6), 539–546.
- (75) Sanosh, K. P.; Chu, M.-C.; Balakrishnan, A.; Kim, T. N.; Cho, S.-J. Preparation and characterization of nano-hydroxyapatite powder using sol-gel technique. *Bulletin of Materials Science* **2009**, *32* (5), 465–470.
- (76) Pusparini, E.; Sopyan, I.; Hamdi, M.; Singh, R. Sodium-doped Hydroxyapatite Nanopowder through Sol-gel Method: Synthesis and Characterization. *Mater. Sci. Forum* **2011**, *694*, 128–132.
- (77) Saranya, K.; Kowshik, M.; Ramanan, S. R. Synthesis of hydroxyapatite nanopowders by sol-gel emulsion technique. *Bulletin of Materials Science* **2011**, *34* (7), 1749–1753.
- (78) Inthong, S.; Tunkasiri, T.; Eitssayeam, S.; Pengpat, K.; Rujijanagul, G. Physical properties and bioactivity of nanocrystalline hydroxyapatite synthesized by a co-precipitation route. *Ceram. Int.* **2013**, *39*, S533–S536.
- (79) Bouyegh, S.; Tlili, S.; Hassani, M.; Mohamed, G.; Oussama, B. Preparation and characteristics of synthesized hydroxyapatite from bovine bones and by co-precipitation method. In *Proceedings of the International Conference on Industrial Engineering and Operations Management*, Monterrey, Mexico, November 3–5, 2021; IEOM Society International: Southfield, MI, 2021; pp 2420–2429.
- (80) Javadinejad, H. R.; Ebrahimi-Kahrizsangi, R. Thermal and kinetic study of hydroxyapatite formation by solid-state reaction. *International Journal of Chemical Kinetics* **2021**, *53* (5), 583–595.
- (81) Pu'ad, N. M.; Haq, R. A.; Noh, H. M.; Abdullah, H.; Idris, M.; Lee, T. Synthesis method of hydroxyapatite: A review. *Mater. Today Proc.* **2020**, *29*, 233–239.
- (82) Mandal, T.; Mishra, B.; Garg, A.; Chaira, D. Optimization of milling parameters for the mechanochemical synthesis of nanocrystalline hydroxyapatite. *Powder technology* **2014**, *253*, 650–656.
- (83) Toriyama, M.; Ravaglioli, A.; Krajewski, A.; Celotti, G.; Piancastelli, A. Synthesis of hydroxyapatite-based powders by mechano-chemical method and their sintering. *Journal of the European Ceramic society* **1996**, *16* (4), 429–436.
- (84) Meejoo, S.; Maneepprakorn, W.; Winotai, P. Phase and thermal stability of nanocrystalline hydroxyapatite prepared via microwave heating. *Thermochimica acta* **2006**, *447* (1), 115–120.
- (85) Jaber, H. L.; Hammood, A. S.; Parvin, N. Synthesis and characterization of hydroxyapatite powder from natural Camelus bone. *Journal of the Australian Ceramic Society* **2018**, *54* (1), 1–10.
- (86) Canillas, M.; Rivero, R.; García-Carrodegas, R.; Barba, F.; Rodríguez, M. A. Processing of hydroxyapatite obtained by combustion synthesis. *Boletín de la Sociedad Española de Cerámica y Vidrio* **2017**, *56* (5), 237–242.
- (87) Lamkhao, S.; Phaya, M.; Jansakun, C.; Chandet, N.; Thongkorn, K.; Rujijanagul, G.; Bangrak, P.; Randorn, C. Synthesis of hydroxyapatite with antibacterial properties using a microwave-assisted combustion method. *Sci. Rep.* **2019**, *9*, 4015.

- (88) Cho, J. S.; Kang, Y. C. Nano-sized hydroxyapatite powders prepared by flame spray pyrolysis. *J. Alloys Compd.* **2008**, *464* (1–2), 282–287.
- (89) Aizawa, M.; Hanazawa, T.; Itatani, K.; Howell, F.; Kishioka, A. Characterization of hydroxyapatite powders prepared by ultrasonic spray-pyrolysis technique. *J. Mater. Sci.* **1999**, *34* (12), 2865–2873.
- (90) Bertran, O.; del Valle, L. J.; Revilla-Lopez, G.; Rivas, M.; Chaves, G.; Casas, M. T.; Casanovas, J.; Turon, P.; Puiggali, J.; Aleman, C. Synergistic Approach to Elucidate the Incorporation of Magnesium Ions into Hydroxyapatite. *Chem. Eur. J.* **2015**, *21* (6), 2537–2546.
- (91) Suchanek, W. L.; Byrappa, K.; Shuk, P.; Riman, R. E.; Janas, V. F.; TenHuisen, K. S. Preparation of magnesium-substituted hydroxyapatite powders by the mechanochemical-hydrothermal method. *Biomaterials* **2004**, *25* (19), 4647–4657.
- (92) Chen, C. W.; Suchanek, W. L.; Shuk, P.; Byrappa, K.; Oakes, C.; Riman, R. E.; Brown, K.; Tenhuisen, K. S.; Janas, V. F. The role of ammonium citrate washing on the characteristics of mechanochemical-hydrothermal derived magnesium-containing apatites. *Journal of Materials Science-Materials in Medicine* **2007**, *18* (7), 1413–21.
- (93) Ren, F.; Leng, Y.; Xin, R.; Ge, X. Synthesis, characterization and ab initio simulation of magnesium-substituted hydroxyapatite. *Acta Biomaterialia* **2010**, *6* (7), 2787–2796.
- (94) Shoba, E.; Lakra, R.; Kiran, M. S.; Korrapati, P. S. 3 D nano bilayered spatially and functionally graded scaffold impregnated bromelain conjugated magnesium doped hydroxyapatite nanoparticle for periodontal regeneration. *Journal of the mechanical behavior of biomedical materials* **2020**, *109*, 103822.
- (95) Ferri, M.; Campisi, S.; Scavini, M.; Evangelisti, C.; Carniti, P.; Gervasini, A. In-depth study of the mechanism of heavy metal trapping on the surface of hydroxyapatite. *Appl. Surf. Sci.* **2019**, *475*, 397–409.
- (96) Alagarsamy, G.; Nithiya, P.; Sivasubramanian, R.; Selvakumar, R. Multi-ionic interaction with magnesium doped hydroxyapatite-zeolite nanocomposite porous polyacrylonitrile polymer bead in aqueous solution and spiked groundwater. *Environ. Pollut.* **2022**, *309*, 119728.
- (97) Ma, X.; Liu, Y.; Zhu, B. Preparation of magnesium-doped nano-hydroxyapatite and its application in drug delivery. *Chin. J. Inorg. Chem.* **2018**, *34* (05), 917–924.
- (98) Ramakrishnan, P.; Nagarajan, S.; Thiruvengatam, V.; Palanisami, T.; Naidu, R.; Mallavarapu, M.; Rajendran, S. Cation doped hydroxyapatite nanoparticles enhance strontium adsorption from aqueous system: A comparative study with and without calcination. *Appl. Clay Sci.* **2016**, *134*, 136–144.
- (99) Lilley, K. J.; Gbureck, U.; Knowles, J. C.; Farrar, D. F.; Barralet, J. E. Cement from magnesium substituted hydroxyapatite. *Journal of Materials Science-Materials in Medicine* **2005**, *16* (5), 455–460.
- (100) Adzila, S.; Sopyan, I.; Bin Abd Shukor, M. H.; Singh, R. Mechanochemical Synthesis of Nanosized Hydroxyapatite Powder and its Conversion to Dense Bodies. *Mater. Sci. Forum* **2011**, *694*, 118–122.
- (101) Adzila, S.; Ramesh, S.; Sopyan, I.; Tan, C. Y.; Hamdi, M.; Teng, W. D. Mechanochemical Synthesis of Magnesium Doped Hydroxyapatite: Powder Characterization. *Applied Mechanics and Materials* **2013**, *372*, 62–65.
- (102) Cacciotti, I.; Bianco, A.; Lombardi, M.; Montanaro, L. Mg-substituted hydroxyapatite nanopowders: Synthesis, thermal stability and sintering behaviour. *Journal of the European Ceramic Society* **2009**, *29* (14), 2969–2978.
- (103) Kang, M.-H.; Jung, H.-D.; Kim, S.-W.; Lee, S.-M.; Kim, H.-E.; Estrin, Y.; Koh, Y.-H. Production and bio-corrosion resistance of porous magnesium with hydroxyapatite coating for biomedical applications. *Mater. Lett.* **2013**, *108*, 122–124.
- (104) Xiong, G.; Nie, Y.; Ji, D.; Li, J.; Li, C.; Li, W.; Zhu, Y.; Luo, H.; Wan, Y. Characterization of biomedical hydroxyapatite/magnesium composites prepared by powder metallurgy assisted with microwave sintering. *Curr. Appl. Phys.* **2016**, *16* (8), 830–836.
- (105) Somasundaram, M.; Uttamchand, N. K.; Annamalai, A. R.; Jen, C. P. Insights on Spark Plasma Sintering of Magnesium Composites: A Review. *Nanomaterials (Basel)* **2022**, *12* (13), 2178.
- (106) Khodaei, M.; Nejatidaneh, F.; Shirani, M. J.; Iyengar, S.; Sina, H.; Savabi, O. Magnesium/Nano-hydroxyapatite Composite for Bone Reconstruction: The Effect of Processing Method. *Journal of Bionic Engineering* **2020**, *17* (1), 92–99.
- (107) Kubásek, J.; Vojtěch, D.; Maixner, J.; Dvorský, D. The effect of hydroxyapatite reinforcement and preparation methods on the structure and mechanical properties of Mg-HA composites. *Science and Engineering of Composite Materials* **2017**, *24* (2), 297–307.
- (108) Del Campo, R.; Savoini, B.; Munoz, A.; Monge, M. A.; Pareja, R. Processing and mechanical characteristics of magnesium-hydroxyapatite metal matrix biocomposites. *Journal of the mechanical behavior of biomedical materials* **2017**, *69*, 135–143.
- (109) Guisbiers, G.; Mejía-Rosales, S.; Leonard Deepak, F. Nanomaterial properties: size and shape dependencies. *J. Nanomater.* **2012**, *2012*, 180976.
- (110) Nakahata, I.; Tsutsumi, Y.; Kobayashi, E. Mechanical Properties and Corrosion Resistance of Magnesium-Hydroxyapatite Composites Fabricated by Spark Plasma Sintering. *Metals* **2020**, *10* (10), 1314.
- (111) Munir, Z. A.; Anselmi-Tamburini, U.; Ohyanagi, M. The effect of electric field and pressure on the synthesis and consolidation of materials: A review of the spark plasma sintering method. *J. Mater. Sci.* **2006**, *41* (3), 763–777.
- (112) Moradi, E.; Ebrahimian-Hosseinabadi, M.; Khodaei, M.; Toghyani, S. Magnesium/nano-hydroxyapatite porous biodegradable composite for biomedical applications. *Materials Research Express* **2019**, *6* (7), 075408.
- (113) Campo, R. D.; Savoini, B.; Muñoz, A.; Monge, M. A.; Garcés, G. Mechanical properties and corrosion behavior of Mg-HAP composites. *Journal of the mechanical behavior of biomedical materials* **2014**, *39*, 238–46.
- (114) Aizenberg, J. New nanofabrication strategies: inspired by biomineralization. *MRS Bull.* **2010**, *35* (4), 323–330.
- (115) Aizenberg, J.; Pokroy, B.; Kang, S. H.; Epstein, A. New nanofabrication strategies: Inspired by biomineralization. In *Abstracts of Papers of the American Chemical Society*; American Chemical Society: Washington, DC, 2009.
- (116) Chen, S.; Shi, Y.; Zhang, X.; Ma, J. Biomimetic synthesis of Mg-substituted hydroxyapatite nanocomposites and three-dimensional printing of composite scaffolds for bone regeneration. *J. Biomed. Mater. Res., Part A* **2019**, *107* (11), 2512–2521.
- (117) Ma, J.; Wang, J.; Ai, X.; Zhang, S. Biomimetic self-assembly of apatite hybrid materials: from a single molecular template to bi-/multi-molecular templates. *Biotechnol. Adv.* **2014**, *32* (4), 744–60.
- (118) Zhao, X.; Yang, Z.; Liu, Q.; Yang, P.; Wang, P.; Wei, S.; Liu, A.; Zhao, Z. Potential Load-Bearing Bone Substitution Material: Carbon-Fiber-Reinforced Magnesium-Doped Hydroxyapatite Composites with Excellent Mechanical Performance and Tailored Biological Properties. *ACS Biomaterials Science & Engineering* **2022**, *8* (2), 921–938.
- (119) Zhang, H.; Li, X.; Wen, J. Preparation and thermal stability of magnesium-doped hydroxyapatite whiskers. *Journal of Synthetic Crystals* **2017**, *46* (07), 1220–1226.
- (120) Wang, X.; Li, X.; Ito, A.; Watanabe, Y.; Sogo, Y.; Hirose, M.; Ohno, T.; Tsuji, N. M. Rod-shaped and substituted hydroxyapatite nanoparticles stimulating type 1 and 2 cytokine secretion. *Colloids and Surfaces B-Biointerfaces* **2016**, *139*, 10–16.
- (121) Sihni, Y.; Yang, H. M.; Park, C. W.; Yoon, I. H.; Kim, I. Post-substitution of magnesium at Ca(I) of nano-hydroxyapatite surface for highly efficient and selective removal of radioactive (90)Sr from groundwater. *Chemosphere* **2022**, *295*, 133874.
- (122) Tampieri, A.; Celotti, G.; Landi, E.; Sandri, M. Magnesium doped hydroxyapatite: Synthesis and characterization. In *Euro Ceramics VIII*; Mandal, H., Övecoglu, L., Eds.; Trans Tech Publications Ltd: Baech, Switzerland, 2004; pp 2051–2054.

- (123) Cox, S. C.; Jamshidi, P.; Grover, L. M.; Mallick, K. K. Preparation and characterisation of nanophase Sr, Mg, and Zn substituted hydroxyapatite by aqueous precipitation. *Materials Science and Engineering: C* **2014**, *35*, 106–114.
- (124) Farzadi, A.; Bakhshi, F.; Solati-Hashjin, M.; Asadi-Eydivand, M.; Osman, N. A. a. Magnesium incorporated hydroxyapatite: Synthesis and structural properties characterization. *Ceram. Int.* **2014**, *40* (4), 6021–6029.
- (125) Šupová, M. Substituted hydroxyapatites for biomedical applications: A review. *Ceram. Int.* **2015**, *41* (8), 9203–9231.
- (126) Tite, T.; Popa, A.-C.; Balescu, L. M.; Bogdan, I. M.; Pasuk, I.; Ferreira, J. M. F.; Stan, G. E. Cationic Substitutions in Hydroxyapatite: Current Status of the Derived Biofunctional Effects and Their In Vitro Interrogation Methods. *Materials* **2018**, *11* (11), 2081.
- (127) Anita Lett, J.; Sagadevan, S.; Léonard, E.; Fatimah, I.; Motalib Hossain, M. A.; Mohammad, F.; Al-Lohedan, H. A.; Paiman, S.; Alshahateet, S. F.; Abd Razak, S. I.; Johan, M. R. Bone tissue engineering potentials of 3D printed magnesium-hydroxyapatite in polylactic acid composite scaffolds. *Artif Organs* **2021**, *45* (12), 1501–1512.
- (128) Swetha, S.; Balagangadharan, K.; Lavanya, K.; Selvamurugan, N. Three-dimensional-poly(lactic acid) scaffolds coated with gelatin/magnesium-doped nano-hydroxyapatite for bone tissue engineering. *Biotechnol. J.* **2021**, *16* (11), No. 2100282.
- (129) Sedghi, R.; Shaabani, A.; Sayyari, N. Electrospun triazole-based chitosan nanofibers as a novel scaffolds for bone tissue repair and regeneration. *Carbohydr. Polym.* **2020**, *230*, 115707.
- (130) Kazimierczak, P.; Kolmas, J.; Przekora, A. Biological Response to Macroporous Chitosan-Agarose Bone Scaffolds Comprising Mg- and Zn-Doped Nano-Hydroxyapatite. *International Journal of Molecular Sciences* **2019**, *20* (15), 3835.
- (131) Dittler, M. L.; Unalan, I.; Grünwald, A.; Beltrán, A. M.; Grillo, C. A.; Destch, R.; Gonzalez, M. C.; Boccaccini, A. R. Bioactive glass (45S5)-based 3D scaffolds coated with magnesium and zinc-loaded hydroxyapatite nanoparticles for tissue engineering applications. *Colloids and Surfaces B-Biointerfaces* **2019**, *182*, 110346.
- (132) Scalera, F.; Palazzo, B.; Barca, A.; Gervaso, F. Sintering of magnesium-strontium doped hydroxyapatite nanocrystals: Towards the production of 3D biomimetic bone scaffolds. *J. Biomed. Mater. Res., Part A* **2020**, *108* (3), 633–644.
- (133) Ahmadzadeh, E.; Talebnia, F.; Tabatabaei, M.; Ahmadzadeh, H.; Mostaghaci, B. Osteoconductive composite graft based on bacterial synthesized hydroxyapatite nanoparticles doped with different ions: From synthesis to in vivo studies. *Nanomedicine* **2016**, *12* (5), 1387–1395.
- (134) Xing, Y.; Zhong, X.; Chen, S.; Wu, S.; Chen, K.; Li, X.; Su, M.; Liu, X.; Zhong, J.; Chen, Z.; Pan, H.; Chen, Z.; Liu, Q. Optimized osteogenesis of porcine bone-derived xenograft through surface coating of magnesium-doped nanohydroxyapatite. *Bioactive Materials* **2023**, *18* (5), 055025.
- (135) Roffi, A.; Kon, E.; Perdisa, F.; Fini, M.; Di Martino, A.; Parrilli, A.; Salamanna, F.; Sandri, M.; Sartori, M.; Sprio, S.; Tampieri, A.; Marcacci, M.; Filardo, G. A Composite Chitosan-Reinforced Scaffold Fails to Provide Osteochondral Regeneration. *International Journal of Molecular Sciences* **2019**, *20* (9), 2227.
- (136) Canullo, L.; Wiel Marin, G.; Tallarico, M.; Canciani, E.; Musto, F.; Dellavia, C. Histological and Histomorphometrical Evaluation of Postextractive Sites Grafted with Mg-Enriched Nano-Hydroxyapatite: A Randomized Controlled Trial Comparing 4 Versus 12 Months of Healing. *Clinical Implant Dentistry and Related Research* **2016**, *18* (5), 973–983.
- (137) Bonany, M.; Pérez-Berná, A. J.; Dučić, T.; Pereiro, E.; Martín-Gómez, H.; Mas-Moruno, C.; van Rijt, S.; Zhao, Z.; Espanol, M.; Ginebra, M. P. Hydroxyapatite nanoparticles-cell interaction: New approaches to disclose the fate of membrane-bound and internalised nanoparticles. *Biomaterials Advances* **2022**, *142*, 213148.
- (138) Zhao, Z.; Espanol, M.; Guillem-Martí, J.; Kempf, D.; Diez-Escudero, A.; Ginebra, M. P. Ion-doping as a strategy to modulate hydroxyapatite nanoparticle internalization. *Nanoscale* **2016**, *8* (3), 1595–607.